Pattern recognition reveals characteristic postprandial glucose changes: Non-individualized meal detection in diabetes mellitus type 1

Konstanze Kölle, Torben Biester, Sverre Christiansen, Anders Lyngvi Fougner, Øyvind Stavdahl

***Abstract*—Accurate continuous glucose monitoring (CGM) is essential for fully automated glucose control in diabetes mellitus type 1. State-of-the-art glucose control systems automatically regulate the basal insulin infusion. Users still need to manually announce meals to dose the prandial insulin boluses. An automated meal detection could release the user and improve the glucose regulation.**

In this study, patterns in the postprandial CGM data are exploited for meal detection. Binary classifiers are trained to recognize the postprandial pattern in horizons of the estimated glucose rate of appearance and in CGM data. The appearance rate is determined by moving horizon estimation (MHE) based on a simple model. Linear discriminant analysis (LDA) is used for classification. The proposed method is compared to methods that detect meals when thresholds are violated.

Diabetes care data from twelve free-living pediatric patients was downloaded during regular screening. Experts identified meals and their start by retrospective evaluation.

The classification was tested by cross-validation. Compared to the threshold-based methods, LDA showed higher sensitivity to meals with a low rate of false alarms. Classifying horizons outperformed the other methods also with respect to time of detection.

The onset of meals can be detected by pattern recognition based on estimated model states and consecutive CGM measurements. No individual tuning is necessary. This makes the method easily adopted in the clinical practice.

***Index Terms*—Artificial pancreas, Continuous glucose monitoring, Diabetes mellitus type 1, Meal detection, Moving horizon estimation.**

I. Introduction

MEAL detection can enable fully automated glucose control in diabetes mellitus type 1. Meal ingestion is followed by characteristic patterns in continuous glucose monitoring (CGM) data that can be exploited for meal detection. Recent clinical studies on closed-loop glucose control (using subcutaneous glucose sensing and insulin administration) have achieved a time in range of 60–80%. While hypoglycemia accounts for only 2–4% of the time with exceeded glucose control limits, 20–30% of the closed loop time is still spent in hyperglycemia [1]. Meals are likely the main reason why the glucose concentration frequently exceeds the upper control limit. Meal announcements are often used to resolve this issue. The patient has to either estimate the size of the insulin bolus directly or the amount of carbohydrates. This is an error-prone challenge for many patients. Safety reasons permit preventive insulin administration by fully automated systems based on probabilities from historical data. Even in bi-hormonal control with insulin and the antagonistic hormone glucagon, preventive insulin administration seems inappropriate due to the risk of system failure. It was demonstrated that meal detection with subsequent insulin bolus administration can improve the outcomes of fully automated closed-loop glucose control [2].

Meals should be detected as early as possible in order to counteract the glucose rise by means of a timely insulin administration. The latency between the administration of insulin into the subcutaneous tissue and the glucose-decreasing effect of insulin, which is also in new ultra-rapid analogues at least 15 min [3], emphasizes the need for an early meal detection. However, the ingestion of food is not the only reason for rising glucose levels; other perturbations may lead to similar glucose curves and, depending on the method, trigger a false meal detection.

Meal detection received increasing attention during the past years. The earlier methods detect a meal based on threshold violations of (occasionally filtered) CGM values. Recently, more complex methods using a model of the glucose-insulin metabolism and data-driven methods were proposed. Most approaches for meal detection utilize the measurements of one CGM device. Meal detection by threshold checking has been suggested with different combinations of checked variables; the raw CGM data is either directly used or revised by removing measurement noise using a linear noise model in a Kalman filter (KF) [4], [5], [6]. Alternatively, the nonlinear Bergman minimal model has been used to estimate the rate of glucose appearance in plasma with an unscented KF (UKF), and meals were detected when this estimate violated an upper threshold [7], [2]. Two redundant glucose sensors were used in a set-up to detect both faults and meals [8]. An UKF is separately applied to the two sensor signals to predict multiple steps of the CGM values; a meal is detected if both estimates simultaneously indicate a positive deviation. Moreover, meal detection based on the cross-covariance between two estimated states of an UKF has been recently proposed [9], [10]. An augmented version of the Bergman model appeared also in a physiologically invariant method [11] where invariant statistics are used to differentiate between effects that can be explained

K. Kölle, A. L. Fougner and Ø. Stavdahl are with the Department of Engineering Cybernetics, Norwegian University of Science and Technology (NTNU), Trondheim, Norway. e-mail: konstanze.koelle@ntnu.no

K. Kölle and S. Christiansen are with the Department of Endocrinology, St. Olav Hospital, Trondheim, Norway.

T. Biester is with Diabetes Center for Children and Adolescents, AUF DER BULT, Hanover, Germany.

Manuscript received Oct 6, 2018; revised Jan 23, 2019; revised Feb 19, 2019; accepted Mar 25, 2019.

by the model with the (lumped) physiological parameters and previous meals and those that must result from a more recent meal. The data-driven fuzzy logic was used to categorize segments of continuously monitored glucose data according to their shape [12], [13].

Many methods for meal detection use combinations of consecutive threshold violations of the sensed glucose concentration and its rate of change as indication for a meal [4], [5], [6]. These threshold-based methods require carefully chosen thresholds. Individual thresholds might be necessary to achieve the right compromise between sensitivity and specificity [14]. A safe tuning of these threshold-based methods is too time-intensive for clinical practice. This might be the reason why the most advanced, commercialized glucose control systems still require manual user input regarding the timing and amount of ingested carbohydrates, whereas basal insulin needs are automated.

Previously suggested methods for meal detection consider only a few of the most current glucose measurements, for example those of the last 15 min [6]. In this paper, we apply methods of pattern recognition to longer horizons of measurements. The aim is to extract the characteristic changes in CGM caused by the onset of meals. In particular, moving horizon estimation (MHE) is used to estimate the rate of glucose appearance [15]. Other estimators such as the Kalman filter update the current estimate based on a single, most recent measurement. The MHE considers a horizon of past glucose measurements at each time step and estimates likewise a horizon of the rate of glucose appearance. At each time step, not only the most recent estimate, but the whole estimated backward horizon is updated when more recent measurements are available. The dynamical changes within the estimated horizons are exploited in the pattern recognition [15]. Both the rate of appearance of glucose in blood estimated with a moving horizon estimation (MHE) and the CGM data directly are used as inputs to the pattern recognition method. The method showed promising performance in a simulation study [15] and is validated on clinical data in this article.

II. Clinical data

Diabetes care data of twelve pediatric patients was included in this study. The clinical data was downloaded at the *Hospital for Children and Adolescents "AUF DER BULT"* in Hanover, Germany, during regular visits. The regional ethical committee (Ethikkommission der Medizinischen Hochschule Hannover) approved the analysis of the anonymized data in this research. Table I contains demographic information of the study population consisting of 8 males and 4 females. The data set consists of CGM measurements from a subcutaneous sensor, administered amounts of basal and bolus insulin, amounts of carbohydrates entered by the patients into the bolus wizard system, alarms, etc. All patients used devices by Medtronic: Enlite 2 sensors, MiniLink or Guardian 2 Link transmitters, and MiniMed pump models. Patients were not advised to change their regular life routines for this study; the data was instead included retrospectively. Therefore, the free-living data shows the normal, non-restricted lifestyle of the patients.

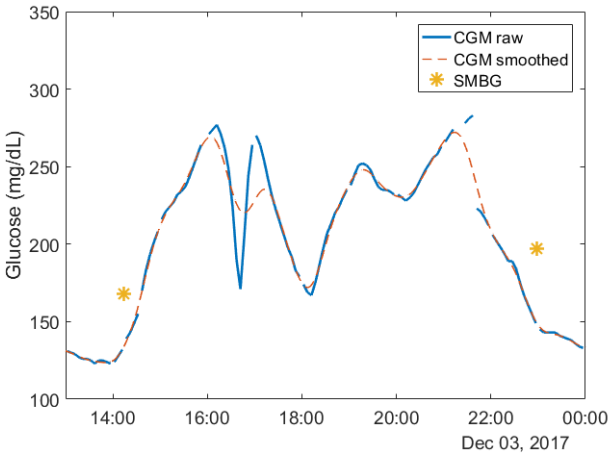

Fig. 1. Raw versus smoothed CGM data. Example with smoothed outliers around 16:45 and replaced missing value at 21:40. Self-monitored blood glucose (SMBG) is also shown.

Since the data set that was not collected for this particular study, meals had to be marked in retrospect based on CGM data and logged information from the insulin infusion pumps. Experienced diabetologists inspected the data and marked meals including an estimation of the timing of prandial insulin. The meals were distinguished into those with boluses either administered before, at or after the meal start. In some occasions, prandial boluses were omitted. A meal was assigned to the pre-meal or post-meal bolus class if the closest meal-related bolus was given within 1 h before or after the start of the glucose increase. If no bolus was used within this period of 2 h, the meal was assigned to have no bolus. The number of marked meals in each class is presented in Table II for each patient. The assessments of the two independent experts were in good agreement with each other.

The amount of ingested carbohydrates at the marked meal times is not reported because this patient-entered information is uncertain. Moreover, the goal of this study was to detect meals causing significant postprandial glucose excursions, the actual amount of carbohydrates is less important in this context.

A. Pre-processing

Missing values disturb the classification. Thus, the raw CGM data has been smoothed using a Kalman filter (KF). The KF implementation by [16] has been used without correction based on finger prick measurements. Besides substituting the missing values, the KF smooths the CGM data. This mainly affects times with high-frequent changes and outliers. Particularly, faults such as spikes that suggest a sudden increase of glucose could be mistaken as meals. The KF was applied to remove non-physiological glucose changes from the data. Such non-physiological changes would compromise the performance of the classifier if they were included in the training set. Figure 1 shows an example where the CGM measurements spike to a value more than 100 mg/dL lower and return to the previous range within one hour. The KF is able to reduce the

TABLE I
DEMOGRAPHIC INFORMATION OF THE STUDY POPULATION CONSISTING OF 12 CHILDREN (8 MALES, 4 FEMALES). REPORTED ARE MEAN VALUES WITH STANDARD DEVIATION IN PARENTHESES. IU: INSULIN UNITS; BW: BODY WEIGHT.

Age [years]	Diabetes duration [years]	HbA1c [%]	Weight [kg]	Size [cm]	BMI [kg/m^2]	Average daily insulin [IU/(kg BW)]
7.3 (4.7)	3.9 (3.1)	7.2 (0.8)	31.6 (21.1)	122.7 (34.3)	18.4 (2.6)	0.8 (0.1)

TABLE II
MARKED MEALS WITH TIMING OF INSULIN BOLUSES RELATIVE TO MEAL ONSET. THE COLUMN 'TOTAL' SUMMARIZES THE NUMBER OF MEALS FOR EACH PATIENT. THE COLUMN 'INCLUDED' REPORTS THE NUMBER OF INCLUDED MEALS THAT DO NOT VIOLATE THE EXCLUSION CRITERIA.

Patient	Number of confirmed meals with Pre-meal bolus	At-meal bolus	Post-meal bolus	No bolus	Total	Included
1	7	17	45	16	85	48
2	4	25	10	12	51	41
3	14	19	39	16	88	57
4	24	11	16	26	77	45
5	6	9	9	42	66	34
6	1	12	14	38	65	29
7	5	5	14	38	62	44
8	4	15	26	41	86	48
9	6	12	23	40	81	56
10	18	19	11	31	79	38
11	9	18	14	16	57	25
12	3	4	7	29	52	27
Sum	101	166	228	345	849	492

spike, thereby reducing the risk of false meal detections caused by such outliers.

B. Construction of training set

We focused on glucose excursions that were caused by meals and that should have been mitigated by (a larger amount of) insulin. These are the meals that should be targeted by an automatic meal detection method. Small meals or snacks that do not cause a significant increase of glucose do not need to be detected because the nominal control system can be assumed to be capable of mitigating their glucose-increasing effect in a sufficient manner. In order to allow us to compare detection times relative to the meal onset, the beginning of the marked meals was adjusted: it was shifted to the first instance (in close proximity to the marked time), where the CGM changed with more than 1 mg/dL/min. If this rate of change was not reached in the 15 min before or after the marked meal, the meal was excluded. Along the same lines, meals that were well compensated by the administered insulin were excluded. Again, the reason for this exclusion is that those meals do not reflect a situation in which an automatic meal detection is needed. An automated method should instead be capable of detecting meals that are not regulated, and also be designed for that purpose. We defined that meals with an increase of at least 40 mg/dL within the first two postprandial hours are not (or only insufficiently) regulated meals. The last column of Table II summarizes the number of included meals that do not violate these criteria.

Classifiers require a comprehensive training set that represents the states to be classified. The classification task for early meal detection is to differentiate between "meal onset" and "no meal onset". The class "meal onset" is defined by the marked meals. The class "no meal onset" was assigned to times when neither meals were confirmed nor the bolus wizard has been used. Times with use of bolus wizard (that were not marked as meal by the experts) were excluded because food might have actually been taken. Therefore, an interval starting 30 min before and ending 60 min after the logged use of the bolus wizard (with an entered carbohydrate amount unequal 0) was omitted.

III. METHODS

A. Methods for meal detection

Two methods using classification of horizons were compared to two methods based on threshold violations. The four implemented methods are:

1) Classification of estimated R_a horizons: The proposed meal detection by classification is based on estimations of the glucose rate of appearance R_a. A version of the Bergman model [17] is used to estimate R_a with a moving horizon estimator. Linear discriminant analysis (Appendix B) is applied to the R_a horizons from MHE. A more detailed description of MHE and LDA can be found in Appendix A and Appendix B, respectively.

The last 20 nodes of the estimated R_a horizons, i.e. a period of the most current 100 min, are used for detection. A horizon with a meal onset falling within the horizon's most current 60 min, i.e. the horizon ends no later than 60 min after meal onset, is designated to the class "meal onset". All others are assigned to the class "no meal onset". Thus, the "meal onset"-class does not cover the whole prandial period. That ensures that the classification is trained to detect the onset of meals. The training, validation and testing is topic of Section III-C.

2) Classification of CGM horizons: Meals are detected by classifying the glucose measurements without running them through an MHE. Not the raw measurements are used, but the smoothed CGM values. The feature matrix with 100 min long horizons is built in the same way as for the classification of the R_a horizons (Appendix B). Also in this case, the LDA classifier is trained following the procedure described in Section III-C.

3) Threshold on current R_a estimate: Meal detection by classification is compared to a method that checks the current R_a estimate against a threshold. A meal is detected if the most current R_a estimate exceeds the threshold. The current estimate at each time step corresponds to the last value of the horizon. In a previous study using the unscented Kalman filter (UKF), meals of various glucose content were detected if the estimated glucose rate of appearance exceeded 2 mg/dL/min [7]. The value of this threshold was not fixed here but tuned according to the protocol in Section III-C.

4) GRID algorithm: The Glucose Rate Increase Detector (GRID) by Harvey et al. [6] applies thresholds to the glucose measurements and its rate of change. The training set of the original study comprised 12 adults with a mean age of 53 years. To adapt the GRID algorithm to the pediatric population of this study, we tuned the thresholds as reported in Section III-C.

B. Performance measures of meal detection

A meal detection is defined as a true positive (TP) when the confirmed meal is detected within 60 min from its start. A false negative (FN) detection occurs if the meal is not detected within this period. Instances of detection out of the first postprandial hour are regarded as false positives (FP) if they do not fulfill at least one of the following criteria:

Use of bolus wizard
: Occasionally, patients used the bolus wizard and entered an amount of carbohydrates at times where the physicians did not mark a meal. Samples in the interval $[-30, +60]$ min around such usage of the bolus wizard were left out because it is uncertain whether the carbohydrates were actually taken and when, or if the bolus wizard was rather used to set a correction bolus.

Marked by physicians
: A detection of a meal that was marked by the experts but excluded according to the criteria inSection III-C is not counted as FP. The FP detection is paused for 30 min after such meal markers.

Missing CGM data
: When CGM data has been missing for more than 2 h, this period (plus 300 min to re-establish full MHE horizons) was excluded. Shorter periods of missing CGM data were included.

Consecutive TP samples are counted as a single TP instance. Likewise, consecutive FPs are counted as one single FP detection. The FP detections were compared per day. For that, the number of FPs was divided by the number of days included in the test data.

Based on TP and FN, the sensitivity S is calculated:

$$S = \frac{TP}{TP + FN}\,. \tag{1}$$

It is unknown whether the patients ate at times beyond the marked. Thus, the examination of true negative (TN) meal detections is omitted and the specificity cannot be evaluated either.

C. Training, validation and tuning procedure

The meal detection by the four different methods is tested in 10 cross-validated Monte Carlo runs. In each run, the data of the 12 subjects is randomly divided into three sets. Each set contains the data of four subjects. The training and validation sets are used to train and tune the methods, while the third set is left out for testing. This test set is used to evaluate the performance of meal detection according to the measures described in Section III-B.

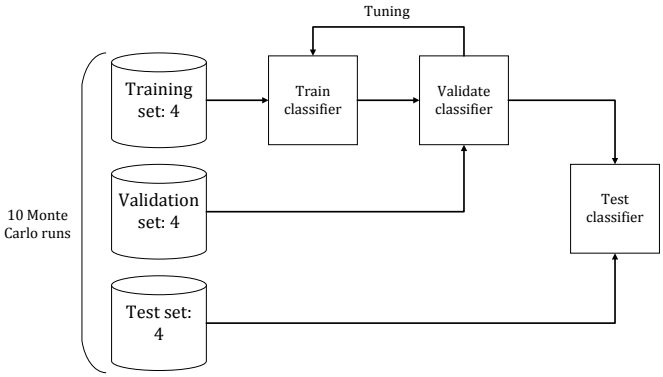

Fig. 2. Procedure of training, validation and testing of classification methods.

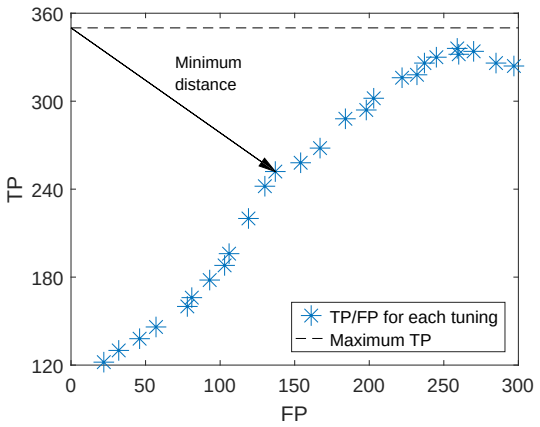

Fig. 3. Illustration of the tuning method by grid search. This example shows the grid search of the threshold tuning on the R_a estimate. The maximum number of TPs is defined by the number of meals in the training set (horizontal, dashed line).

1, 2) Classification of R_a and CGM horizons: The LDA classifier is used to investigate meal detection by classification of R_a and CGM horizons. Figure 2 illustrates the procedure of training, validation and testing of the classifiers. The classifiers are fitted to the training set and then applied to the validation set. A grid search is conducted to find the parameters of the LDA classifier that minimize the classification error of the validation set. The classification error is rated by means of the mean squared error between the real and the predicted response vector. The classifier tuning that results in the lowest mean squared error is chosen and tested on the test set. The meal detection performance of these tests are eventually compared to the meal detection by the other methods.

The parameters of the LDA classifier are varied as follows: $\delta = 10^{[-15,-12,\cdots,3]}$, $\gamma = [0, 0.1, \cdots, 1]$.

3, 4) Threshold on R_a estimate and GRID algorithm: The classification error is unsuited to evaluate the performance of the other two methods because they are not trained to fit the response vector. Instead, the goal during tuning is to detect the meals in accordance with the measures defined in Section III-B. The number of TP and FP meal detections are used as criteria to find the best thresholds. An ideal meal detection would detect all meals and not cause any false alarm (maximum TP, no FP). The Euclidean distance between this

This article has been accepted for publication in a future issue of this journal, but has not been fully edited. Content may change prior to final publication. Citation information: DOI 10.1109/JBHI.2019.2908897, IEEE Journal of Biomedical and Health Informatics

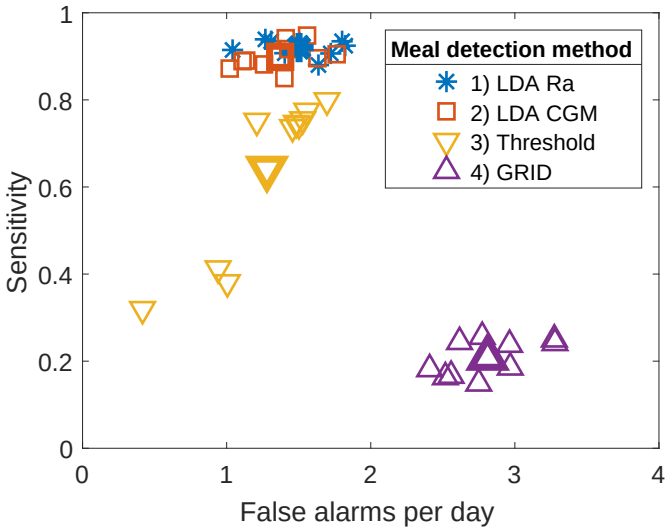

Fig. 4. Number of true positive and false negative meal detections. One marker indicates the results of one Monte Carlo run. The bold marker is the average of the Monte Carlo runs.

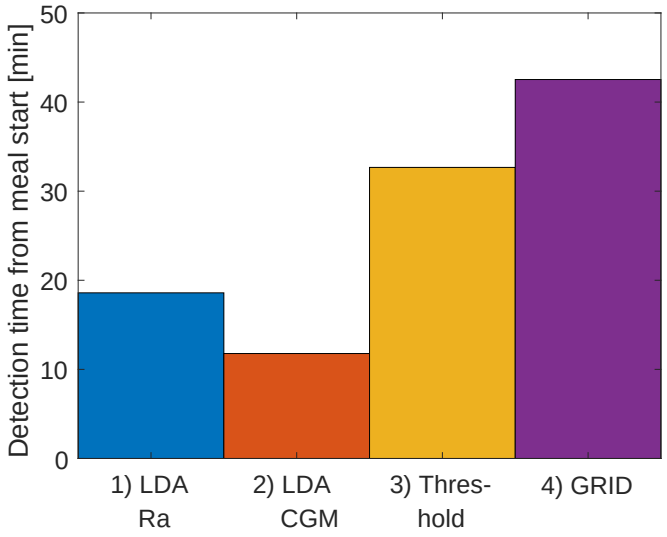

Fig. 5. Time of detection after meal start. One bar indicates the average time over all Monte Carlo runs.

ideal point and the one achieved with a particular tuning is used to quantify the performance. Figure 3 illustrates that the tuning with the minimum distance to the ideal point is chosen. Both the training and the validation sets were combined for the tuning of the R_a threshold and the parameters of the GRID algorithm.

The following thresholds on the R_a estimate were tested: $[1.5, 1.6, \ldots, 4]$ mg/dL/min.

Three parameters of the GRID algorithm were tuned: the minimum glucose concentration (G_{min}), the rate of change over the last three measurements ($\Delta G_{\text{min},3}/\Delta t$) and the rate of change over the last two measurements ($\Delta G_{\text{min},2}/\Delta t$). The first tuning parameter that imposes a minimum CGM value to trigger meal detection was varied in the range $[110, 120, \ldots, 150]$ mg/dL. The two latter were varied with a step size of 0.1 mg/dL/min; $\Delta G_{\text{min},3}/\Delta t$ between 1.2 and 1.7 mg/dL/min and $\Delta G_{\text{min},2}/\Delta t$ between 1.3 and 1.8 mg/dL/min. Should the current glucose concentration exceed G_{min} and change faster than defined by one of the rate parameters, a meal is detected.

IV. Results

Figure 4 presents the performance by means of sensitivity towards meals and false alarms per day. Each cross-validated Monte Carlo run is represented by one marker. The bold markers in Fig. 4 indicate the average over all Monte Carlo runs with the same method. Tables IV to VII in the appendix contain the numerical values for each Monte Carlo run.

The sensitivity of classification of R_a horizons by LDA lies above 0.88 with less than 2 false alarms per day. A similar rate of false positive detections occurs when LDA is applied to the CGM horizons. The sensitivity towards meals is also similar compared to the classification of R_a horizons.

A decreased sensitivity is observed for the thresholding of the most current R_a estimate. While the sensitivities spread over a wider range, the thresholding of R_a results in an average sensitivity of 0.64 and up to 1.7 false alarms daily. The sensitivity of the GRID algorithm to the meals in the test set was 0.2 with 2.4 to 3.3 false positives per day. Thus, the GRID algorithm showed overall the worst performance in this study with the current set-up.

The time of detection from meal start is compared in Fig. 5. One bar represents the average over the 10 Monte Carlo runs with the particular method. The fastest average detection of 12 min was achieved by classifying CGM data by LDA. The classification of R_a horizons by LDA follows with 19 min. Meal detection by checking the most current R_a estimate against a threshold resulted in an average detection time of 33 min. The GRID algorithm revealed meals on average within 43 min.

In total, both classification methods based on analyzing horizons detected more meals in shorter time than the threshold-based methods.

V. Discussion

This study demonstrates that the classification of estimated states or even CGM data can be used for fast meal detection. The comparative methods are used here as representatives of threshold-based methods. They were tuned to ensure comparability but may perform better when tuned differently.

The classification of estimated R_a horizons combines advantages of model-based and data-driven methods. The underlying model forces the estimated rate of glucose appearance to be physiologically meaningful (within the limits of the model), while the classification avoids to define a single decisive threshold. The estimator model should describe the general dynamics of the BGL, but it does not need to accurately map the glucose-insulin dynamics. Instead, the classification can compensate for structural mismatch between model and the real metabolism. Even if an estimated state does not conform with its real equivalent, the estimates will be classified as those in similar situations of the training data. MHE considers

a whole horizon of original measurements in each iteration. Other estimators such as the Kalman filter emphasize the most current measurement and summarize the information of all previous measurements in the covariance of the most current estimate [18]. Moreover, constraints on states and parameters are explicitly considered by the MHE.

The classification of CGM horizons was as sensitive to meals as the classification of R_a horizons. Together with slightly fewer false alarms and an on average 7 min faster detection, the moving horizon estimation might be unnecessary but time-consuming. Further studies should investigate the benefits that an estimation step could add to the robustness of the method. A different or adapted estimator model is one possible attempt.

In practical use, threshold-based methods necessitate careful tuning to fit the purpose. Moreover, a threshold used for sensible decisions in diabetes management should be revised on a regular basis to consider adaptations of lifestyle, weight changes, or an overall improved or diminished diabetes therapy. For safety reasons, this tuning should preferably be done under supervision of a health care-provider. The classification method (LDA), on the other hand, could adapt automatically: The user would need to confirm the onset of meals occasionally. This could be requested in a similar way as finger prick measurements to calibrate the CGM. The effect of erroneous inputs can be diminished by a large training set, whereas the consequences of a poorly chosen threshold would be harder to compensate. To restrict the training set to a practical size and to keep it up to date, the oldest meals could be replaced after a defined period. Although it is a strength if a method does not require individualization, the performance might increase if the method is trained using only data from the patient whose meals shall be detected. Individual meal dynamics would be considered in that way. To test this hypothesis, a sufficient amount of data for one patient is needed.

The data was not particularly designed for this study but originates from unrestricted, free-living conditions. Meals were therefore marked retrospectively by experienced endocrinologists. Given the high variability among persons and within the same patient [19], the timing of carbohydrate intake is somewhat uncertain and may have led to a few false assessments. This was considered by careful definition of meal-free periods in the sets used to train and validate the classifiers (Section II-B), as well as in the analysis of FP meal detections (Section III-B). On the other hand, the free-living character of the data set is a strength, as it shows the realistic variability of clinical data and confirms the results of the previous simulation study [15] on real data.

A data set collected under more controlled conditions should be used to confirm the findings of this pilot study and further evaluate meal detection by classification. In particular, a data set with exact timing of the meal start and with information about the type and amount of the ingested food should be collected. One could also assess the possibility to estimate an appropriate insulin bolus for the detected meal, or estimating the meal type.

Other events leading to increased BGL may degrade the performance of meal detection. Those situations, that require a similar treatment as meals do, are not necessarily problematic. For example, some of the patients used an insulin pump function that suspends insulin infusion upon predicted hypoglycemia at normal BGL. Manual interference with this feature by oral carbohydrate intake, intended to treat hypoglycemia, during suspended insulin infusion may immediately lead to higher BGL [20]. This is not a critical situation per se because insufficient insulin has been administered compared to the ingested carbohydrates. Contrary to this, an excursion that appears like a meal in the beginning but is then followed by a significant drop can be dangerous if insulin is automatically dosed. A careful trade-off between early meal detection and certainty about the actual presence of a meal is necessary. Physical activity may be falsely classified as meal because mixed and anaerobic exercises can result in rising BGL [21]. A reliable differentiation between meals and exercise should be investigated. An activity monitor integrated into the system could help to prevent such false meal detections [22].

The classification of meals can be extended to fault detection. The constraints on states and parameters in the MHE force the R_a horizons to physiological values and changes. If the method finds it physiologically impossible that an observed change of glucose concentration was caused by a meal, no solution will be found, or unusual dynamics of the states are used to explain this situation. This might be exploited for detection of system faults.

Furthermore, the robustness and safety of meal detection could be increased by a voting scheme that requires two or more consecutive samples to be classified as a meal. This more conservative approach is safer but will delay the meal detection time. Another option is to only trigger meal detection when the glucose concentration exceeds a minimum value [6].

VI. Conclusion

The proposed meal detection by classification of horizons of the estimated rate of glucose appearance or CGM data successfully revealed meals in a clinical data set. The classification of horizons of the estimated rate leads to slightly more true and fewer false detections, compared to the classification of the CGM horizons. The time of detection after meal start is promising at the same time.

The advantages of the proposed methods are:

- only the commonly available CGM data is used as input;
- no individual tuning is needed;
- adjustments to changing physiology can be done similar to CGM calibrations;
- and the same method could be used for differentiation between meal sizes if different classifiers are trained accordingly.

Appendix

A. Moving Horizon Estimation (MHE)

The moving horizon estimator for meal detection has been described previously [15].

As a model-based technique, the MHE is based on a set of ordinary differential equations (ODEs) that describe the system:

$$\dot{\boldsymbol{x}}(t) = \tilde{\boldsymbol{f}}(\boldsymbol{x}(t), \boldsymbol{u}(t)) \tag{2a}$$
$$\boldsymbol{y}(t) = \boldsymbol{h}(\boldsymbol{x}(t)) \tag{2b}$$

with the vectors of differential states $\boldsymbol{x} \in \mathbb{R}^{n_x}$, inputs $\boldsymbol{u} \in \mathbb{R}^{n_u}$, and outputs $\boldsymbol{y} \in \mathbb{R}^{n_y}$.

An augmented version of the non-linear model by Bergman et al. [17] was chosen to describe the glucose-insulin dynamics. The model has originally two states, the glucose concentration in plasma G (mg/dL) and the action of insulin X (1/min). The rate of appearance of glucose in plasma R_a (mg/dL/min) and the insulin sensitivity S_I (ml/U/min) are added to the state vector. The glucose appearance in plasma R_a is modeled by a first order Markov process, while the insulin sensitivity S_I is assumed constant. The resulting model for the augmented states $\boldsymbol{x} = [G, X, R_a, S_I]^T$ is:

$$\dot{\boldsymbol{x}}(t) = \begin{bmatrix} -S_G G(t) - X(t)G(t) + S_G G_b + R_a(t) \\ -p_2 X(t) + p_2 S_I(t)\,(I(t) - I_b) \\ -R_a/\tau \\ 0 \end{bmatrix} \tag{3}$$

$$y(t) = G(t)\,. \tag{4}$$

The plasma glucose concentration G is the only measurement y. Diffusion dynamics of glucose from plasma to the SC tissue is not described in order to restrict the dimensionality of the model. The SC measurements are instead substituted for the plasma concentration in the measurement equation, Eq. (4). Along the same lines, the absorption of insulin from the SC tissue into the plasma is not modeled but the insulin concentration in plasma I (pmol/L) remains as input.

The continuous equations in Eq. (2) must be discretized to get a finite dimensional problem that can be solved. The direct collocation method was used for discretization.

$$\underset{\boldsymbol{x}_j, \boldsymbol{w}_j, \boldsymbol{v}_j}{\text{minimize}} \quad J \tag{5a}$$
$$\text{s. t.} \quad \boldsymbol{x}_{j+1} = \boldsymbol{f}(\boldsymbol{x}_j, \boldsymbol{u}_j) + \boldsymbol{w}_j \tag{5b}$$
$$j = k - N + 1, ..., k - 1$$
$$\boldsymbol{y}_j = \boldsymbol{h}(\boldsymbol{x}_j) + \boldsymbol{v}_j \tag{5c}$$
$$j = k - N + 1, ..., k$$
$$\boldsymbol{x}_{j,\min} \leq \boldsymbol{x}_j \leq \boldsymbol{x}_{j,\max} \tag{5d}$$
$$j = k - N + 1, ..., k\,.$$

All states and the measurements are subject to noise and disturbances. This is indicated in the discretized model (Eq. (5)) where unknown disturbances are accommodated by the additive process noise $\boldsymbol{w}_j \in \mathbb{R}^{n_x}$ and the measurement noise $\boldsymbol{v}_j \in \mathbb{R}^{n_y}$.

The MHE solves the optimization problem by minimizing the cost function J. At each time step k, a window of N past measurements $\{\boldsymbol{y}_{k-N+1}, ..., \boldsymbol{y}_k\}$ is provided to the MHE. The MHE estimates the states $\{\boldsymbol{x}_{k-N+1}, ..., \boldsymbol{x}_k\}$ that best explain the given measurements. The optimized state values $\boldsymbol{x}_j$ must fulfill the process and measurement equations in (5b) and (5c), respectively. The lower and upper bounds in (5d) constrain the state estimates additionally. The control variables $\{\boldsymbol{u}_{k-N}, ..., \boldsymbol{u}_{k-1}\}$ are set to their known values at time k.

The objective function (Eq. (5a)) was chosen to explicitly consider both process and measurement noise vectors, $\boldsymbol{w}_j$ and $\boldsymbol{v}_j$:

$$J = \|\boldsymbol{x}_{k-N+1} - \bar{\boldsymbol{x}}_{k-N+1}\|^2_{P^{-1}_{k-N+1}} \tag{6a}$$
$$+ \sum_{j=k-N+1}^{k-1} \|\boldsymbol{w}_j\|^2_{R^{-1}} \tag{6b}$$
$$+ \sum_{j=k-N+1}^{k} \|\boldsymbol{v}_j\|^2_{Q^{-1}}\,. \tag{6c}$$

The first term of Eq. (6a) represents the arrival cost which considers the confidence in the initial estimate $\bar{\boldsymbol{x}}_{k-N+1}$ (first state within the estimation horizon) by means of the estimated error covariance matrix $P_{k-N+1} \in \mathbb{R}^{n_x \times n_x}$. The second and third terms penalize deviations from the process $\boldsymbol{f}(\boldsymbol{x}_j, \boldsymbol{u}_j)$ (Eq. (6b)) and the measurement equations $\boldsymbol{h}(\boldsymbol{x}_k)$ (Eq. (6c)), respectively.

As time passes, the confidence in the initial state may change as well and the arrival cost needs to be updated. Here, a smoothing update of the initial state $\bar{\boldsymbol{x}}_{k-N+1}$ and its covariance P_{k-N+1} was chosen [23]. By tuning the matrices $R \in \mathbb{R}^{n_x \times n_x}$ and $Q \in \mathbb{R}^{n_y \times n_y}$, the magnitudes of process and measurement noise are weighted.

The non-linear problem was implemented with CASADi [24] in Matlab and solved using IPOPT [25].

Estimation set-up: With the motivation of detecting meals, it is assumed that the insulin infusion is close to the basal rate that keeps the glucose concentration stable. On that assumption, the actual value of I has minor impact on the estimation. The basal glucose concentration G_b and the basal insulin concentration I_b have been set to 36 mg/dL and 0 pmol/L, respectively. The remaining parameters are not individualized either. Descriptions of these generic parameters, the used values and their origin are provided in Table III.

TABLE III
PARAMETER VALUES USED IN THE ESTIMATOR MODEL (EQ. (3)).

Parameter		Description
S_G	$1.4 \cdot 10^{-2}\,\text{min}^{-1}$ [26]	Glucose effectiveness
p_2	$3.0 \cdot 10^{-2}\,\text{min}^{-1}$ [26]	Rate constant of insulin action
τ	40 min [27]	Meal absorption time constant
$S_{I,\text{nom}}$	$8.56 \cdot 10^{-4}$ ml/U/min [28]	Nominal insulin sensitivity

A sampling time of 5 min is chosen as it is the most common sampling rate of CGM devices. The optimization problem is constructed at time samples 5 min apart from each other over the whole horizon. These samples are called nodes. The number of nodes in a horizon of e.g. 300 min is thus $N = 300\,\text{min}/5\,\text{min} = 60$.

The initial state (i.e. $\bar{\boldsymbol{x}}_{k-N+1}$ and P^{-1}_{k-N+1} in (6) at $k = 1$) was defined as $\bar{\boldsymbol{x}}_0 = \left[y_0, 10^{-4}, 0, S_{I,\text{nom}}\right]^T$ with an initial covariance $P_0 = I$. The covariance P of the initial state is part of the arrival cost calculation; a smoothing update based on an extended Kalman filter (EKF) was chosen [23]. The process and measurement covariances used in this EKF scheme were $\tilde{Q} = \text{diag}\,(10, 10, 1, 1)$ and $\tilde{R} = 100$, respectively.

The weighting matrices in the MHE cost function (6) were $Q = \text{diag}\,(50, 10, 10, 1)^2$ for the process noise and $R = 10^2$ for the measurement noise. States and noise vectors were bounded as

$$\begin{bmatrix} \boldsymbol{x}_{\text{min}} \\ \boldsymbol{w}_{\text{min}} \\ \boldsymbol{v}_{\text{min}} \end{bmatrix} \leq \begin{bmatrix} \boldsymbol{x} \\ \boldsymbol{w} \\ \boldsymbol{v} \end{bmatrix} \leq \begin{bmatrix} \boldsymbol{x}_{\text{max}} \\ \boldsymbol{w}_{\text{max}} \\ \boldsymbol{v}_{\text{max}} \end{bmatrix} , \tag{7}$$

in which the inequalities should be interpreted elementwise, with

$$\boldsymbol{x}_{\text{min}} = \left[36, -10^{-2}, 0, 0.5 \cdot S_{I,\text{nom}}\right]^T , \tag{8a}$$

$$\boldsymbol{x}_{\text{max}} = \left[300, 10^{-2}, 10, 2 \cdot S_{I,\text{nom}}\right]^T , \tag{8b}$$

$$\boldsymbol{w}_{\text{min}} = \left[-10^{-4}, -10^{-8}, 0, -10^{-8}\right]^T , \tag{8c}$$

$$\boldsymbol{w}_{\text{max}} = \left[10^{-4}, 10^{-8}, \text{inf}, 10^{-8}\right]^T , \tag{8d}$$

$$\boldsymbol{v}_{\text{min}} = -10^8 \quad \text{and} \tag{8e}$$

$$\boldsymbol{v}_{\text{max}} = 10^8 . \tag{8f}$$

Constraints on the process noise ensure that the glucose rate of appearance cannot be negative and that the insulin sensitivity changes only slowly. The MHE has been tuned to the data of one day for one subject different from those included. The tuning aimed to minimize the error between the measured and the estimated glucose concentration.

B. Classification using pattern recognition by linear discriminant analysis

The goal of pattern recognition is to discriminate between different classes within a data set. As we want to differentiate between "meal onset" and "no meal onset", we focus on binary classification. Based on characteristic features, binary classification algorithms separate observations into two classes. The pattern recognition methods apply supervised learning, i.e. they are trained on a training set with known classes.

As features we use the estimated glucose rate of appearance R_a and the CGM data, $x \in \{R_a, G\}$. One type of features is arranged in the feature matrix $X \in \mathbb{R}^{L \times N}$:

$$X = \begin{bmatrix} x(k-N) & \dots & x(k-1) & x(k) \\ x(k-N-1) & \dots & x(k-2) & x(k-1) \\ \vdots & \ddots & \vdots & \vdots \\ x(k-N-L) & \dots & x(k-1-L) & x(k-L) \end{bmatrix} . \tag{9}$$

Subsequent observations may overlap by $L-1$.

An output vector $Y \in \mathbb{R}^N$ defines the known classes by assigning either 0 or 1 to the corresponding columns in Eq. (9). A 0 indicates that the observation in X contains "no meal onset", while 1 indicates a "meal onset":

$$Y = [0, 0, 0, 1, 1, 1, 1, 0, 0, \dots] . \tag{10}$$

The example in Eq. (10) indicates a meal onset for the observations 4–7, columns 4–7 of the feature matrix Eq. (9).

Linear discriminant analysis (LDA) is one of the standard classification methods in pattern recognition. LDA applies Bayes' theorem to assign posterior probabilities that an observation with the features x belongs to the class "meal onset". A new observation is assigned to the class for which the linear discriminant function is maximum [29].

The Matlab function `fitcdiscr` was used to train an LDA model. The tuning of its parameters, the linear coefficient threshold *delta* and the regularization parameter *gamma*, is discussed in Section III-C.

C. Numerical results

TABLE IV
MEAL DETECTION BY CLASSIFICATION OF R_a HORIZONS. RESULTS OF EACH MONTE CARLO RUN.

Monte Carlo run	Sensitivity (Eq. (1))	False alarms per day	Time of detection after meal start [min]
1	0.91	1.40	19.17
2	0.92	1.82	19.62
3	0.93	1.31	17.78
4	0.91	1.72	17.68
5	0.93	1.51	18.35
6	0.93	1.80	18.82
7	0.91	1.04	19.70
8	0.93	1.51	19.86
9	0.94	1.27	17.06
10	0.88	1.64	17.87
Average	0.92	1.50	18.59

TABLE V
MEAL DETECTION BY CLASSIFICATION OF CGM HORIZONS. RESULTS OF EACH MONTE CARLO RUN.

Monte Carlo run	Sensitivity (Eq. (1))	False alarms per day	Time of detection after meal start [min]
1	0.88	1.26	13.15
2	0.95	1.56	13.36
3	0.89	1.11	11.52
4	0.90	1.63	9.29
5	0.92	1.43	10.92
6	0.90	1.76	11.19
7	0.87	1.02	12.73
8	0.94	1.41	13.41
9	0.89	1.14	11.10
10	0.85	1.40	11.12
Average	0.90	1.37	11.78

TABLE VI
MEAL DETECTION BY THRESHOLD ON CURRENT R_a ESTIMATE. RESULTS OF EACH MONTE CARLO RUN.

Monte Carlo run	Sensitivity (Eq. (1))	False alarms per day	Time of detection after meal start [min]
1	0.74	1.46	31.75
2	0.41	0.94	36.00
3	0.75	1.21	30.91
4	0.77	1.56	30.96
5	0.32	0.42	38.67
6	0.38	1.00	36.90
7	0.74	1.50	30.41
8	0.75	1.48	30.57
9	0.80	1.70	30.19
10	0.76	1.53	30.30
Average	0.64	1.28	32.67

ACKNOWLEDGMENT

The study was financed by The Liaison Committee for Education, Research and Innovation in Central Norway (project no. 46075403) and partly by the Research Council of Norway (project no. 248872) and the Centre for Digital Life Norway.

TABLE VII
MEAL DETECTION BY GRID ALGORITHM. RESULTS OF EACH MONTE CARLO RUN.

Monte Carlo run	Sensitivity (Eq. (1))	False alarms per day	Time of detection after meal start [min]
1	0.19	2.97	44.72
2	0.24	2.62	44.05
3	0.16	2.52	43.80
4	0.24	3.28	47.05
5	0.17	2.56	37.71
6	0.15	2.75	39.80
7	0.24	2.96	43.08
8	0.18	2.41	36.43
9	0.26	2.77	44.17
10	0.25	3.27	44.50
Average	0.21	2.81	42.53

REFERENCES

[1] S. Christiansen, A. L. Fougner, Ø. Stavdahl, K. Kölle, R. Ellingsen, and S. M. Carlsen, "A review of the current challenges associated with the development of an artificial pancreas by a double subcutaneous approach," *Diabetes Therapy*, vol. 8, pp. 1–18, 2017.

[2] K. Turksoy, I. Hajizadeh, S. Samadi, J. Feng, M. Sevil, M. Park, L. Quinn, E. Littlejohn, and A. Cinar, "Real-time insulin bolusing for unannounced meals with artificial pancreas," *Control Engineering Practice*, vol. 59, no. C, pp. 159–164, February 2017.

[3] T. Heise, T. R. Pieber, T. Danne, L. Erichsen, and H. Haahr, "A pooled analysis of clinical pharmacology trials investigating the pharmacokinetic and pharmacodynamic characteristics of fast-acting insulin aspart in adults with type 1 diabetes," *Clinical Pharmacokinetics*, vol. 56, no. 5, pp. 551–559, May 2017.

[4] E. Dassau, B. W. Bequette, B. A. Buckingham, and F. J. Doyle, III, "Detection of a meal using continuous glucose monitoring implications for an artificial β-cell," *Diabetes care*, vol. 31, no. 2, pp. 295–300, 2008.

[5] H. Lee and B. W. Bequette, "A closed-loop artificial pancreas based on model predictive control: Human-friendly identification and automatic meal disturbance rejection," *Biomed Signal Process Control*, vol. 4, no. 4, pp. 347–354, 2009.

[6] R. A. Harvey, E. Dassau, H. Zisser, D. E. Seborg, and F. J. Doyle, "Design of the glucose rate increase detector a meal detection module for the health monitoring system," *J Diabetes Sci Technol*, p. 1932296814523881, 2014.

[7] K. Turksoy, S. Samadi, J. Feng, E. Littlejohn, L. Quinn, and A. Cinar, "Meal detection in patients with type 1 diabetes: A new module for the multivariable adaptive artificial pancreas control system," *IEEE Journal of Biomedical and Health Informatics*, vol. 20, no. 1, pp. 47–54, 2016.

[8] Z. Mahmoudi, K. Nørgaard, N. K. Poulsen, H. Madsen, and J. B. Jørgensen, "Fault and meal detection by redundant continuous glucose monitors and the unscented kalman filter," *Biomedical Signal Processing and Control*, vol. 38, pp. 86–99, 2017.

[9] C. M. Ramkissoon, P. Herrero, J. Bondia, and J. Vehi, "Meal detection in the artificial pancreas: Implications during exercise," *IFAC PapersOnLine*, vol. 50, no. 1, pp. 5462–5467, July 2017.

[10] C. Ramkissoon, P. Herrero, J. Bondia, and J. Vehi, "Unannounced meals in the artificial pancreas: Detection using continuous glucose monitoring," *Sensors (Switzerland)*, vol. 18, no. 3, 2018.

[11] J. Weimer, S. Chen, A. Peleckis, M. R. Rickels, and I. Lee, "Physiology-invariant meal detection for type 1 diabetes," *Diabetes Technology & Therapeutics*, vol. 18, no. 10, pp. 616–624, October 2016.

[12] S. Samadi, K. Turksoy, I. Hajizadeh, J. Feng, M. Sevil, and A. Cinar, "Meal detection and carbohydrate estimation using continuous glucose sensor data," *Biomedical and Health Informatics, IEEE Journal of*, vol. 21, no. 3, pp. 619–627, May 2017.

[13] S. Samadi, M. Rashid, K. Turksoy, J. Feng, I. Hajizadeh, N. Hobbs, C. Lazaro, M. Sevil, E. Littlejohn, and A. Cinar, "Automatic detection and estimation of unannounced meals for multivariable artificial pancreas system," *Diabetes technology & therapeutics*, February 2018.

[14] K. Kølle, A. L. Fougner, and Ø. Stavdahl, "Impact of sensing and infusion site dependent dynamics on insulin bolus based meal compensation," *IFAC-PapersOnLine*, vol. 50, no. 1, pp. 7749 – 7755, 2017.

[15] K. Kölle, A. L. Fougner, and Ø. Stavdahl, "Meal detection based on non-individualized moving horizon estimation and classification," in *2017 IEEE Conference on Control Technology and Applications (CCTA)*, Aug 2017, pp. 529–535.

[16] O. M. Staal, S. Saelid, A. L. Fougner, and Ø. Stavdahl, "Kalman smoothing for objective and automatic preprocessing of glucose data," *IEEE Journal of Biomedical and Health Informatics*, vol. PP, no. 99, pp. 1–1, 2018.

[17] R. N. Bergman, L. S. Phillips, and C. Cobelli, "Physiologic evaluation of factors controlling glucose tolerance in man: measurement of insulin sensitivity and beta-cell glucose sensitivity from the response to intravenous glucose," *The Journal of clinical investigation*, vol. 68, no. 6, p. 1456, 1981.

[18] D. G. Robertson, J. H. Lee, and J. B. Rawlings, "A moving horizon-based approach for least-squares estimation," *AIChE Journal*, vol. 42, no. 8, pp. 2209–2222, 1996.

[19] Y. C. Kudva, R. E. Carter, C. Cobelli, R. Basu, and A. Basu, "Closed-loop artificial pancreas systems: physiological input to enhance next-generation devices," *Diabetes Care*, vol. 37, no. 5, pp. 1184–1190, 2014.

[20] T. Biester, O. Kordonouri, M. Holder, K. Remus, D. Kieninger-Baum, T. Wadien, and T. Danne, ""Let the Algorithm Do the Work": Reduction of Hypoglycemia Using Sensor-Augmented Pump Therapy with Predictive Insulin Suspension (SmartGuard) in Pediatric Type 1 Diabetes Patients," *Diabetes Technology & Therapeutics*, vol. 19, no. 3, pp. 173–182, 2017.

[21] M. C. Riddell, I. W. Gallen, C. E. Smart, C. E. Taplin, P. Adolfsson, A. N. Lumb, A. Kowalski, R. Rabasa-Lhoret, R. J. Mccrimmon, C. Hume, F. Annan, P. A. Fournier, C. Graham, B. Bode, P. Galassetti, T. W. Jones, I. S. Millán, T. Heise, A. L. Peters, A. Petz, and L. M. Laffel, "Exercise management in type 1 diabetes: a consensus statement," *The Lancet Diabetes & Endocrinology*, vol. 5, no. 5, pp. 377–390, May 2017.

[22] K. Turksoy, L. Quinn, E. Littlejohn, and A. Cinar, "Monitoring and fault detection of continuous glucose sensor measurements," in *ACC, Chicago, US-IL*, 2015, pp. 5091–5096.

[23] M. J. Tenny and J. B. Rawlings, "Efficient moving horizon estimation and nonlinear model predictive control," in *Proceedings of the 2002 American Control Conference*, vol. 6, 2002, pp. 4475–4480.

[24] J. Andersson, "A general-purpose software framework for dynamic optimization," PhD Thesis, Arenberg Doctoral School, KU Leuven, 2013.

[25] A. Wächter and L. T. Biegler, "On the implementation of an interior-point filter line-search algorithm for large-scale nonlinear programming," *Mathematical Programming*, vol. 106, no. 1, pp. 25–57, 2006.

[26] C. Dalla Man, A. Caumo, and C. Cobelli, "The oral glucose minimal model: estimation of insulin sensitivity from a meal test," *IEEE Trans. Biomed. Eng.*, vol. 49, no. 5, pp. 419–429, 2002.

[27] R. Hovorka, V. Canonico, L. J. Chassin, U. Haueter, M. Massi-Benedetti, M. O. Federici, T. R. Pieber, H. C. Schaller, L. Schaupp, and T. Vering, "Nonlinear model predictive control of glucose concentration in subjects with type 1 diabetes," *Physiological measurement*, vol. 25, no. 4, p. 905, 2004.

[28] C. Dalla Man, A. Caumo, R. Basu, R. Rizza, G. Toffolo, and C. Cobelli, "Minimal model estimation of glucose absorption and insulin sensitivity from oral test: validation with a tracer method," *American journal of physiology. Endocrinology and metabolism*, vol. 287, no. 4, p. E637, 2004.

[29] G. James, "An introduction to statistical learning : with applications in r," 2013.